Automated Respiration Detection from Neonatal Video Data

Ninah Koolen[1,2], Olivier Decroupet[1], Anneleen Dereymaeker[3], Katrien Jansen[3], Jan Vervisch[3], Vladimir Matic[1,2], Bart Vanrumste[1,2,4], Gunnar Naulaers[3], Sabine Van Huffel[1,2]and Maarten De Vos[5,6]

[1]*Department of Electrical Engineering (ESAT), division STADIUS, University of Leuven, Leuven, Belgium*

[2]*iMinds-KU Leuven Medical IT Department, Leuven, Belgium*

[3]*Department of Development and Regeneration, University of Leuven, Leuven, Belgium*

[4] *Faculty of Engineering Technology, AdvISe Technology Lab, University of Leuven campus Geel, Geel, Belgium*

[5]*Department of Psychology, University of Oldenburg, Oldenburg, Germany*

[6]*Institute of Biomedical Engineering, Department of Engineering Science, University of Oxford, Oxford, U.K.*

Keywords: Automated Respiration Detection, Neonatal Care, Polysomnography, Video, Optical Flow Algorithm, Eulerian Video Magnification.

Abstract: In the interest of the neonatal comfort, the need for noncontact respiration monitoring increases. Moreover, home respiration monitoring would be beneficial. Therefore, the goal is to extract the respiration rate from video data included in a polysomnography. The presented method first uses Eulerian video magnification to amplify the respiration movements. A respiration signal is obtained through the optical flow algorithm. Independent component analysis and principal component analysis are applied to improve the signal quality, with minor enhancement of the signal quality. The respiratory rate is extracted as the dominant frequency in the spectrograms obtained using the short-time Fourier transform. Respiratory rate detection is successful (94.12%) for most patients during quiet sleep stages. Real-time monitoring could possibly be achieved by lowering the spatial and temporal resolutions of the input video data. The outline for successful video-aided detection of the respiration pattern is shown, thereby paving the way for improvement of the overall assessment in the NICU and application in a home-friendly environment.

1 INTRODUCTION

In neonatal care, respiration monitoring is of viable importance. Monitoring the respiration rate facilitates the diagnosis of a number of disorders, like apnea. Neonates normally show respiratory rates around 50-60 breaths per minute. The respiration pattern of the infant changes based on the development of the respiratory system and possible disorders. Three general respiration patterns are observed in neonates: synchronous, simple retraction and see-saw (Miller and Behrle, 1953). They define the phase difference between the chest and the abdomen expansion during breathing. The incidence of these respiratory patterns varies with the age of the neonate. The respiratory system of preterm infants is not fully developed yet; they are therefore more susceptible to show apnea or periodic respiration. Apnea is defined by the cessation of the respiratory airflow, whereas periodic breathing is characterized by groups of respiratory movements interrupted by small intervals of apnea.

Nowadays, most techniques used to monitor the respiration are complex and obtrusive, like polysomnography. Multiple methods to monitor the respiration rate without using a polysomnography have been developed (Al-Khalidi et al., 2011). Most recently, numerous techniques aiming for a contactless respiration monitoring have been investigated. A lot of these attempts involve sensors integrated under or into the mattress (Folke et al., 2003). Methods based on acoustic and radar detection exist as well, using the Doppler principle to estimate motions induced by the respiration (Li et al., 2013). Similar techniques use time-of-flight cameras to estimate the frequency of the chest movements during respiration (Penne et al., 2008). Some attempts at visual detection make use of infrared camera to detect motions in the scene (Abbas and Heiman, 2009). The infrared cameras

Koolen N., Decroupet O., Dereymaeker A., Jansen K., Vervisch J., Matic V., Vanrumste B., Naulaers G., Van Huffel S. and De Vos M..
Automated Respiration Detection from Neonatal Video Data.
DOI: 10.5220/0005187901640169
In *Proceedings of the International Conference on Pattern Recognition Applications and Methods* (ICPRAM-2015), pages 164-169
ISBN: 978-989-758-077-2

estimate the skin temperature of the patient which can be related to inspiration and expiration of air during breathing.

Other methods focus on processing images obtained from regular cameras. Differences between frames are used to estimate movements in the video data (Tan et al., 2010). Based on the same principle, the optical flow algorithm can be applied to an image sequence (Nakjima, 2001). These techniques are however developed for older subjects and do not mention successful respiration detection during sleep in a dark setting. The same problem is present with techniques based on the detection of colour changes (Kwon et al., 2012; Aarts et al., 2013). These can provide a very accurate detection of the respiration and the heart rate but they rely on a good illumination of the face of the patient which is unrealistic for sleep monitoring.

Most of these techniques require the use of sophisticated devices, which can be expensive and difficult to set up in a home environment. This paper presents an algorithm to automatically extract the neonatal respiratory rate from video data during deep sleep stages. The required equipment consists of a simple camera and a computer. Breathing movements are magnified in the specific frequency band using Eulerian video magnification, and further processed with the optical flow algorithm to extract a respiration signal. In addition, with ICA and PCA we have aimed to optimize the respiration detection. Using Short-Time Fourier Transformation, a respiration rate is extracted and compared to the control signal by means of cross-correlation.

2 METHODS

2.1 Data Acquisition

Two types of data are acquired for this study. Both video and the respiration signals are obtained during a polysomnography. The dataset included long-term video-EEG recordings of 7 preterm infants with a postmenstrual age of 33-40 weeks. Two patients were labelled with periodic breathing based on visually detection of at most 10 seconds non-breathing intervals. The protocol was approved by the ethics committee of the University Hospitals of Leuven, Belgium. The respiratory effort is measured using two bands, one placed around the thorax of the patient, the other around the abdomen. Each band contains a piezoelectric transducer measuring its extension as the patient breathes in and out. The video data is acquired with a simple camera placed above or near the bed of the baby in different set-ups. All videos are recorded in .wmv format and have the same size: 720x576 pixels. The video images are converted to the .avi format, which works with a constant frame rate. RGB values are changed into gray values. As the objective is to detect respiration from these videos, the region of interest is limited to the body of the baby. All video images are manually cropped to contain only the chest and abdomen region as indicated in Figure 1. This operation has two advantages: a lowering of the noise levels and a reduction of the computation time.

Figure 1: Screenshot of the video image in a dark setting. Region of interest (ROI) is manually selected.

2.2 Data Processing

The recorded video data is processed in multiple steps. First, specific motions in the video are amplified using Eulerian video magnification. The movements are then extracted from the video data with an optical flow algorithm. The output from the optical flow is subsequently adapted in order to obtain a signal of which the quality can be assessed in comparison with the control signals.

2.2.1 Eulerian Video Magnification

Small, sometimes even imperceptible, variations in video images can be amplified to make them visible to the human eye (Wu et al., 2012). Eulerian video magnification amplifies colour changes and small motions in a specified frequency band. The magnification is performed in an Eulerian way. Namely, the algorithm tracks and amplifies changes in pixel intensity values over time. A constant illumination of the scene is therefore necessary.

The framework of video magnification contains both spatial and temporal processing steps. The first one is the spatial decomposition of the video. This creates an image pyramid for each frame, each level of this so-called pyramid contains a specific band of spatial frequencies (Choi et al., 2008). Temporal processing is applied on each spatial band. A bandpass filter is used to extract the temporal frequency band of interest [0.5-2 Hz], which is multiplied by the magnification factor α[=15] and added back to the original signal. The value of α cannot be taken too high, since the noise level will be significantly increased in this way. We describe the principles of motion magnification using a one-dimensional signal. The intensity variation is defined at a certain position *x* over time as *I(x,t)*. A direct generalization to two dimensions is possible. Under condition of translational motion, a displacement function *d(t)* can be used to represent the change in intensity values (formula 1). Magnification to enlarge the respiration is represented in formula 2. Finally, the spatial pyramid is collapsed to create the output video data.

$$I(x,t) = f\big(x + d(t)\big) \text{ with } I(x,0) = f(x) \quad (1)$$

$$I(x,t) = f(x + (1+\alpha) * d(t)) \quad (2)$$

2.2.2 Optical Flow

Optical flow is the distribution of apparent velocities of movement patterns in the image, arising from the relative motion between the viewer and the objects (Horn and Schunck, 1981). Multiple approaches exist to relate motion in the images by calculating the optical flow (Fleet and Weiss, 2006; O'Donovan, 2005). The optical flow is estimated using the partial derivatives I_x, I_y and I_t which represent the difference in brightness between two images. For this purpose, the sum of the Laplacians of the flow velocities u and v, respectively in horizontal and vertical direction, are approximated. These estimates are used to set up the total error function due to assumptions of smoothness and constant brightness. This total error has to be minimized in order to find suitable values for the optical flow velocity (u, v). The optimization gives two equations in u and v from which the flow velocity can be computed using the local average velocities $\bar{u}$ and $\bar{v}$ (formula 3 and 4). a^2 is the weighing factor between the two assumption errors. This optimization is often computed iteratively (Horn and Schunck, 1981).

$$\left(a^2 + I_x^2 + I_y^2\right) * u = \left(a^2 + I_y^2\right) * \bar{u} - I_x * I_y * \bar{v} - I_x * I_t \quad (3)$$

$$\left(a^2 + I_x^2 + I_y^2\right) * v = \left(a^2 + I_x^2\right) * \bar{v} - I_x * I_y * \bar{u} - I_y * I_t \quad (4)$$

A one dimensional respiration signal is retrieved by summing all flow values frame by frame. Each sample represents the total amount of horizontal or vertical flow in the corresponding frame (Sun et al., 2008). In addition, we have compared the obtained signal with the signal obtained by taking only a percentage of the horizontal and vertical optical flow values, e.g. summing only the smallest 50% of the absolute flow values. In case the thorax and the abdomen do not expand simultaneously, a selection of the smallest flow values removes the largest expansion and the largest noise components. Figure 2 shows this signal and its control signal (abdomen strain) for patient 7.

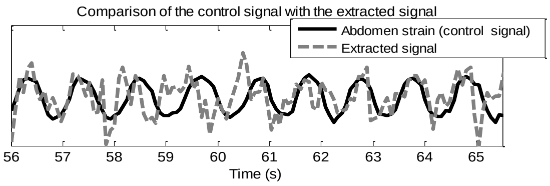

Figure 2: Sum of the 50% smallest vertical optical flow values and abdomen control signal for patient 7.

2.3 Signal Analysis

The frequency content of the signals, obtained by summing the optical flow values of each frame, is analysed with the short-time Fourier transform (STFT). These signals can have a low signal-to-noise ratio, making respiration detection difficult. Independent component analysis (ICA) and principal component analysis (PCA) are performed to improve the signal quality.

2.3.1 Short-Time Fourier Transform

The STFT results in a two-dimensional array representing the frequency components in function of time. The respiratory rate can be extracted from the spectrogram taking the mean of the dominant frequencies in a sliding window of 5, 10 or 20 seconds. A shorter window allows following the variations of the respiration rate more precisely. However, a longer window is preferable when dealing with a signal of lower quality where the respiration rate is not continuously dominant in the frequency spectrum. Furthermore, longer windows are less sensitive to artefacts. Figure 3 shows a spectrogram obtained by the STFT of a four minutes segment for patient 7.

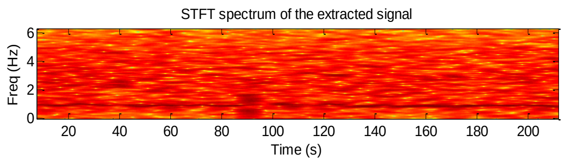

Figure 3: STFT of the sum of the 50% smallest vertical optical flow values for patient 7.

2.3.2 Independent Component Analysis

ICA is a widely used method to perform blind source separation. ICA can be used to separate the respiration pattern from other movement sources or noise in the video images by searching for a set of statistically independent signals among the signal mixtures. The video images are separated into four equal parts and on each part the respiration extraction methods are applied. In this way, we obtain four signal mixtures which will serve as input for ICA.

2.3.3 Principal Component Analysis

PCA is used to extract the most important modes of variation from complex datasets. A signal with a higher signal-to-noise ratio should be reconstructed using only the most important modes of variation of the signal, leaving out the less significant ones. The components with the largest eigenvalues accounting for 98% of the variance are used to reconstruct the signal.

2.3.4 Cross-correlation

The cross-correlation computes the correlation for every time-lag between the extracted respiration signal and the control signal, sliding one signal along the other. The correlation value retained here is the maximal correlation in an interval of 1 second around the zero time-lag. This allows to compensate for a possibly small time-lag between the two signals, e.g. between the thorax control signal and the abdomen expansion picked up in the video image. The correlation value computed in this way is an indicator of the similarity between the control respiration signals and the extracted signal of the video image. The respiration estimate is however sensitive to noise and artefacts, leading to low correlation values given motion artefacts are present.

3 RESULTS AND DISCUSSION

Table 1 shows the correlation between each signal obtained from the optical flow algorithm, ICA or PCA and the corresponding control signal. For each patient, the vertical or horizontal optical flow values are used based on the position of the camera. A percentage of optical flow values is taken as well in the comparison. The effect of this selection is rather small, but generally leads to better results in spite of simultaneous expansions of thorax and abdomen. The 50% flow values in smallest absolute value are selected to serve as an input for both ICA and PCA. Only the ICA and PCA signals for patient 7 give really high correlation values for patients without periodic respiration. This can be explained by the very regular respiration rate and the lack of movement artefacts for this patient. Both patients with periodic respiration (patients 3 and 4) show larger correlation values than the other patients. This is due to the numerous periods of apnea where no motion is detected. As the extracted and control signal have very small values during the apnea periods, the correlation is high (figure 4). On the contrary, the correlation between bursting respiration periods is of a smaller order and comparable to other patients.

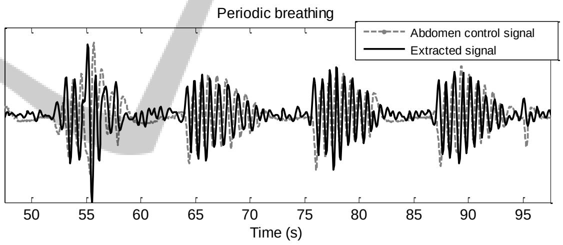

Figure 4: Periodic breathing: comparison between the abdomen control signal and the sum of 50% smallest optical flow values.

Reconstruction of the signal with principal component analysis provides the best result in five out of seven cases. For the two other patients, the best signal is obtained through independent component analysis. However, the difference in correlation between the ICA and PCA signals are

Table 1: Correlation between the control signal and the signals obtained from the optical flow, independent component analysis and principal component analysis. Best results in bold.

	100% vertical	50% vertical	100% horizontal	50% horizontal	ICA	PCA
Patient 1	0.031	0.035	**0.081**	0.076	**0.065**	0.061
Patient 2	0.069	0.074	0.119	**0.129**	0.144	**0.167**
Patient 3	0.408	0.419	0.516	**0.535**	0.155	**0.532**
Patient 4	**0.502**	0.493	0.114	0.122	0.463	**0.495**
Patient 5	0.042	**0.047**	0.042	0.035	0.051	**0.059**
Patient 6	**0.152**	0.143	0.087	0.072	0.122	**0.161**
Patient 7	0.128	**0.142**	0.058	0.066	**0.705**	0.645

Table 2: Correlation between respiratory rate extracted from the control signal and the signal obtained by the optical flow algorithm and after applying ICA and PCA. PR indicates periodic respiration.

	Respiration rate from sum of optical flow values	Respiration rate from ICA estimate	Respiration rate from PCA reconstruction
Patient 1	0.909	0.893	0.907
Patient 2	0.949	0.929	0.955
Patient 3	PR	PR	PR
Patient 4	PR	PR	PR
Patient 5	0.913	0.875	0.903
Patient 6	0.942	0.943	0.933
Patient 7	0.993	0.999	0.998

small for both patients, assuming a preference to use PCA.

Table 2 shows the correlation between the respiratory rates extracted by STFT from the control signal and the signals used for table 1. For each patient, the signal with the highest correlation to the control signal is used, as well as the best estimates obtained using ICA and PCA. The extracted respiration rate is quantized in intervals of 0.1 Hz, since an exact value of the respiratory rate is not needed. Conversely, abrupt changes in the respiration rate are more important to detect. The maximal error introduced by this step is 0.05 Hz, which is insignificant. Physical respiration changes will still be apparent in the quantized respiratory rate. The upside of the quantization is an easier comparison between the rate extracted from both signals and a higher similarity value assuming a small difference between the rates. Both patient 3 and patient 4 have a periodic respiration pattern (PR). This makes an estimation of the breathing rate impossible because of the apnea periods interrupting the respiration.

Correlation values for the respiration rate are in a higher order than for the mutual comparison of the signals themselves due to the selected frequency band in the STFT and the quantization of the respiratory rate.

4 CONCLUSIONS

Using Eulerian video magnification and an optical flow algorithm, we are capable to detect the respiratory rate of newborn infants from video data. Moreover, the breathing frequency can be found by computing the STFT on the extracted signal. The developed method is a first step to detect apnea intervals and periodic breathing during sleep, only based on a simple video registration. Provided the video is not suffering from too many non-respiration related movements, apnea can be detected by the absence of any movement with simple thresholding. The same principle can be used to identify periodic respiration.

However, the computation time to extract a respiration signal is rather high, due to the optical flow algorithm. The computation time can already be significantly reduced by lowering the resolution of the image. The results of the respiration detection are not significantly affected by half the resolution. A reduction of the number of frames per seconds of the input video is another way to decrease the computation time. The respiration rate of newborns is almost never above 1 Hz. Therefore, it should be possible to extract the respiration from the video recordings while lowering the number of frames per second under the 12.5 used here. Combining these two modifications could lead to a significant reduction of the computation time.

The position of the camera relative close to the infant and its bed has to be standardized. For example, a good suggestion would be to place it near the feet on the bed while looking down on the infant at an angle of approximately 45 degrees. In that way, only vertical optical flow values should be taken into account. There would be no or only a small projection on the horizontal axis. Consequently, optimization of the other steps would be possible taking the camera position into account. In addition, the chest and abdomen region of the infant should be visible for the camera. Respiration detection is possible when a thin blanket covers the baby, but not when its body is made completely invisible by a thick blanket.

Nevertheless, the method for respiration detection introduced in this text has a number of advantages on the other techniques used for respiration monitoring of neonates. First, it does not require any piece of equipment to be in contact with the infant. This increases the comfort level of the baby in addition to avoidance of skin irritation and other reactions to the equipment in contact with the patient. The other advantage is the simplicity of the required equipment. The video images used here are standard resolution images captured by a normal camera. The processing only requires a computer. This combination is less expensive than some of the other devices used to monitor the respiration rate from a distance. This simple equipment is also easy to use and could be used in a home environment as well. Home monitoring is more comfortable for the patient and its parents, but it is also less expensive and allows the hospital to take care of another patient instead of the one being monitored at home. In conclusion, this setup is a first step improving the neonatal assessment regarding the vital sign of respiration.

ACKNOWLEDGEMENTS

Research supported by:
Research Council KUL: GOA/10/09 MaNet, CoE PFV/10/002 (OPTEC); PhD/Postdoc grants;
Flemish Government: IWT: projects: TBM 110697-NeoGuard; PhD/Postdoc grants;
Belgian Federal Science Policy Office: IUAP P7/19/ (DYSCO)
EU: ERC Advanced Grant: BIOTENSORS (n° 339804).

REFERENCES

Aarts, L. A., Jeanne, V., Cleary, J. P., Lieber, C., Nelson, J.S., Bambang Oetomo, S., Verkruysse, W., 2013. Non-contact heart rate monitoring utilizing camera photoplethysmography in the neonatal intensive care unit - a pilot study. In *Early Human Development*, 89(12): p. 943-948.

Abbas, A. and Heiman, K., 2009. Non-contact respiratory.
monitoring based on real-time IR-thermography. In *IFMBE Proceedings*, 25(4): p. 1306–1309.

Al-Khalidi, F.Q., Saatchi, R., Burke, D., Elphick, H., and.
Tan, S., 2011. Respiration rate monitoring methods: a review. In *Pediatric pulmonology*, 46(6): p. 523–529.

Choi, J., Jeon,W. J., and Lee, S-C., 2008. Spatio-temporal pyramid matching for sports videos. In *Proceeding of the first ACM international conference on Multimedia information retrieval.* New York, USA: p. 291–297.

Fleet, D. and Weiss, Y., 2006. Optical flow estimation. In *Handbook of Mathematical Models in Computer Vision*: p. 239–258.

Folke, M., Cernerud, L., Ekström, M., and Hök, B., 2003. Critical review of non-invasive respiratory monitoring in medical care. In *Medical & biological engineering & computing*, 41(4): p. 377–383.

Horn, B. K. and Schunck, B. G., 1981. Determining optical flow. In *Artificial Intelligence*, 17(1-3): p. 185–203.

Kwon, S., Kim, H., and Park, K. S., 2012. Validation of heart rate extraction using video imaging on a builtin camera system of a smartphone. In *Proceedings of the Annual International Conference of the IEEE Engineering in Medicine and Biology Society, EMBS*. San Diego, USA: p. 2174–2177.

Li, C., Lubecke, V., Boric-Lubecke, O., and Lin, J., 2013. A review on recent advances in Doppler radar sensors for noncontact healthcare monitoring. In *IEEE Transactions on microwave theory and techniques*, 61(5): p. 2046–2060.

Miller, H. and Behrle, F., 1953. Changing patterns of respiration in newborn infants. In *Pediatrics*, 12(2): p. 141–150.

Nakjima, K., 2001. Development of real-time image sequence analysis for evaluating posture change and respiratory rate of a subject in bed. In *Physiological Measurement*, 22(3): p. 21–28.

O'Donovan, P., 2005. Optical Flow: Techniques and Applications. In *International Journal of Computer Vision*, p. 1–26.

Penne, J., Schaller, C., Hornegger, J., and Kuwert, T., 2008. Robust real-time 3D respiratory motion detection using time-of-flight cameras. In *International Journal of Computer Assisted Radiology and Surgery*, 3(5): p. 427–431.

Sun, D., Roth, S., Lewis, J., and Black, M., 2008. Learning optical flow. In *Computer Vision ECCV, Lecture Notes in Computer Science*, 5304: p. 83-97.

Tan, K., Saatchi, R., Elphick, H., and Burke, D., 2010. Real-time vision based respiration monitoring system. In *Proceeding of the seventh IEEE IET International Symposium on Communication Systems, Networks and Digital Signal Processing.* Newcastle, UK: p. 770–774.

Wu, H.-y., Rubinstein, M., Shih, E., and Freeman, W., 2012. Eulerian Video Magnification for Revealing Subtle Changes in theWorld. In *Proceedings of ACM Transactions on Graphics*, 31: p. 1–8.